Analysis of ^{6}He Coulomb breakup in the complex scaling method

Takayuki Myo and Kiyoshi Katō
Division of Physics, Graduate School of Science, Hokkaido University, Sapporo 060-0810, Japan

Shigeyoshi Aoyama
Information Processing Center, Kitami Institute of Technology, Kitami 090, Japan

Kiyomi Ikeda
RI-Beam Science Laboratory, RIKEN (The Institute of Physical and Chemical Research), Wako, Saitama 351-0198, Japan
(Received 5 January 2001; published 20 April 2001)

The transition strength for Coulomb breakup of ^{6}He into $^4\mathrm{He}+n+n$ three-body unbound states is studied in the framework of the complex scaling method (CSM). We propose a method to analyze the three-body unbound states in which CSM is utilized to decompose the three-body transition strengths into resonance and continuum components. We calculate the contributions of $E1$ and $E2$ transitions, not only from three-body resonances, but also from two-body ''$^5\mathrm{He}+n$'' and three-body ''$^4\mathrm{He}+n+n$'' continuum states. From the calculated strength distributions, we discuss the characteristic structures of ^{6}He in the positive energy region, and also the Coulomb breakup mechanism of ^{6}He. We show that the two-body ''$^5\mathrm{He}+n$'' component is dominant in the total Coulomb breakup cross section.

DOI: 10.1103/PhysRevC.63.054313 PACS number(s): 21.10.Pc, 21.60.Gx, 25.60.Gc

I. INTRODUCTION

The development of radioactive beams provides us with many interesting phenomena of unstable nuclei near the drip lines [1–3]. The most typical example is the discovery of a neutron halo structure in several neutron-rich nuclei such as ^{6}He, ^{11}Li, and ^{11}Be [1,2]. One of the common features of unstable nuclei is the weak binding; the neutron halo nuclei have extremely small binding energies against one- or two-neutron emission. This property of halo nuclei indicates a local breaking of the density and the binding-energy saturations observed in stable nuclei. In unstable nuclei, most of the excited states are unbound; resonances and continuum states. Here we define resonances and continuum states as the eigenstates belonging to discrete and continuum spectra, respectively, obtained with given boundary conditions. In some of the drip line nuclei, even the ground states are resonances. It is expected that the weakly bound halo states have a strong influence on the properties of unbound states. The soft-dipole giant resonance [4,5] is one of the most interesting problems concerning a characteristic excitation mode arising from the weak-binding energy of neutron halo nuclei.

The weak-binding energy of unstable nuclei is also responsible for large breakup cross sections. Through breakup reactions involving neutron halo nuclei, one obtains important information not only about the ground state properties, but also about the fundamental excitation mechanism of unstable nuclei above the threshold energy. In particular, when a high-Z nucleus such as Pb is used as a target, the Coulomb interaction is considered to give a large contribution to the breakup cross reaction. In such a case, we can learn electromagnetic properties such as the soft-dipole resonance from the Coulomb breakup reaction.

Many experimental data on Coulomb breakup reactions have been obtained so far for one-neutron halo nuclei such as $^{11}\mathrm{Be}\,(^{10}\mathrm{Be}+n)$ [6] and $^{19}\mathrm{C}\,(^{18}\mathrm{C}+n)$ [7], and two-neutron halo nuclei such as $^6\mathrm{He}\,(^4\mathrm{He}+n+n)$ [8] and $^{11}\mathrm{Li}\,(^9\mathrm{Li}+n+n)$ [9–11]. The result of ^{11}Be on the Pb target shows a low energy enhancement in the $E1$ transition strength distribution of the two-body breakup reaction. The dipole enhancement observed just above the breakup threshold energy has been explained by a large low-momentum component in the ground state that has a spatially extended one-neutron distribution characteristic of the halo structure [6]. On the other hand, breakup reactions involving two-neutron halo nuclei, which have a core$+n+n$ three-body structure, provide us with richer information on the strength distribution of various kinds of the three-body configurations. From the structure of the cross section, not only the dipole resonance but also other kinds of resonances or continuum effects have been discussed for ^{6}He [8] and ^{11}Li [9–11]. To see the neutron-neutron and the neutron-core correlations in the halo state, breakup reactions have been studied in experimental observations [8–14] of neutron-neutron and neutron-core components in breakup cross section. Furthermore, it is interesting to investigate experimentally the reaction mechanism of direct three-body breakup or sequential breakup through two-body processes.

From the theoretical side, it is necessary to treat weakly bound states, resonances, and also continuum states, simultaneously to investigate breakup reactions. Since there is no difficulty in the treatment of two-body problems, one-neutron halo nuclei, especially the ^{11}Be nucleus, have been investigated in detail [15,16]. However, although many useful methods such as the Faddeev method, the hyperspherical harmonics approach, and the sophisticated variational method [17] have been developed and applied to the $^4\mathrm{He}+n+n$ and $^9\mathrm{Li}+n+n$ systems, we are still having difficult problems, in the description of three-body breakup reactions, to take into account the effects of three-body resonances and binary components such as $^5\mathrm{He}+n$ in ^{6}He. Danilin *et al.* [18] investigated the $E1$ transition strength in Coulomb

breakup reactions of ^{6}He into ^{4}He$+n+n$ unbound states using the hyperspherical harmonics approach. Their result of the strength distribution shows a low energy enhancement and a shoulderlike structure, but no 1^- resonance is obtained. On the other hand, Cobis *et al.* [19] discussed a resonancelike structure caused by 1^- resonances in ^{6}He by applying the method similar to that of Danilin *et al.* There are some conflicts in the theoretical understanding of the Coulomb breakup of ^{6}He. It is therefore necessary to solve these problems and to obtain a correct understanding of breakup reactions involving ^{6}He that is the simplest and the most typical Borromean nucleus.

In our previous papers [20,21], we have shown that the complex scaling method (CSM) [22] is a very useful method to solve many-body resonances and weakly bound states. For ^{6}He, using a three-body ^{4}He$+n+n$ model with CSM, Aoyama *et al.* [20] discussed the spectroscopy of the low excitation energy region including the halo structure of the ground state. In the present paper, we develop the investigation of the three-body unbound structure of ^{6}He by using CSM. For this purpose, we carefully study the structure of the transition strength distribution in the three-body Coulomb breakup reaction of ^{6}He, by paying attention not only to the contribution of resonances but also to the contribution of continuum states.

About CSM, there have been many studies of resonances for several light stable and unstable nuclei [20,21,23–32]. In those studies, however, interest was focused on resonances only. On the other hand, we have shown that CSM is applicable to discuss physical quantities associated with unbound states including resonances and continuum states, such as transition strengths [33–35]. In our previous paper [35], transition strengths of two-body unbound states such as the ^{10}Be$+n$ system, are exactly decomposed into resonance and continuum components, and we discussed which component contributes to the strength distribution explicitly. The decomposition of the strengths based on the extended completeness relation (ECR) proposed by Berggren [36] is performed reasonably in the framework of CSM [34,35]. Using this approach, we discuss the structure of the strengths without any ambiguity to distinguish resonance and continuum states.

In Sec. II, we calculate the wave function of ^{6}He within a ^{4}He$+n+n$ three-body model and explain CSM, ECR and how to decompose the transition strength. In Sec. III, we decompose the $E1$ and $E2$ transition strengths into the various breakup processes. From the results, we discuss which components dominate the obtained total strength and the structure of ^{6}He in the positive energy region through the transition strength. A summary is given in Sec. IV.

II. METHOD

A. Three-body model of ^{6}He

We describe ^{6}He with a ^{4}He$+n+n$ three-body model as shown in Ref. [20]. Here we briefly recapitulate the important properties of the model. The Hamiltonian of the model is the same as in Ref. [20] except for the introduction of a three-body interaction:

$$H=\sum_{i=1}^{3} t_i - T_G + \sum_{i=1}^{2} V_{\alpha n}(\boldsymbol{r}_i) + V_{nn} + V^3_{\alpha nn} + \lambda |\phi_{PF}\rangle\langle\phi_{PF}|, \tag{1}$$

where t_i and T_G are kinetic energies of each particle and the center of mass of the three-body system, respectively. A relative coordinate between ^{4}He and each valence neutron is given by $\boldsymbol{r}_i$. The ^{4}He core cluster is assumed to have $(0s)^4$-closed configuration described by a harmonic oscillator wave function with the length parameter $b_c=1.4$ fm that reproduces the experimental charge radius of ^{4}He. The two-body interactions $V_{\alpha n}$ and V_{nn} are given by the so-called KKNN potential [37] for ^{4}He-n and the so-called Minnesota potential [38] for n-n, respectively. These potentials well reproduce the low-energy scattering data of each two-body system. The three-body ^{4}He-n-n interaction $V^3_{\alpha nn}$ is introduced to fit the binding energy of the ground state as is explained later. The last term $\lambda |\phi_{PF}\rangle\langle\phi_{PF}|$ presents a projection operator to remove the Pauli forbidden states [$(0s)$ state in this case] from the ^{4}He-n relative motion [39], and λ is taken as 10^6 MeV in this calculation.

The weak-binding motion of valence neutrons around the ^{4}He core must be solved accurately on the basis of recent developments of few-body problems. We employ here a variational method, the so-called hybrid-TV model [5,20,40,41], where relative wave functions of ^{4}He$+n+n$ are expanded on basis states of the cluster orbital shell model (COSM; V type) [42,43], and on the additional basis of the extended cluster model (ECM; T type) [5,40,41] for the 0^+ states. The wave function of the three-body model is expressed as follows:

$$\Phi^{J^\pi}(^6\mathrm{He}) = \Phi(^4\mathrm{He})\chi^{J^\pi}(nn), \tag{2}$$

$$\chi^{J^\pi}(nn) = \begin{cases} \chi_V^{J^\pi}(\boldsymbol{\xi}_V) & (\text{V type for } J^\pi \neq 0^+) \\ \chi_V^{J^\pi}(\boldsymbol{\xi}_V) + \chi_T^{J^\pi}(\boldsymbol{\xi}_T) & (\text{hybrid TV for } 0^+). \end{cases} \tag{3}$$

Here, $\chi^{J^\pi}_{V,T}(\boldsymbol{\xi}_{V,T})$ express the wave functions of two valence neutrons, and $\boldsymbol{\xi}_V$ and $\boldsymbol{\xi}_T$ are V-type and T-type coordinate sets, respectively, of the relative motion in the three-body system. The radial component of each relative wave function is expanded with a finite number of Gaussian functions centered at the origin, and the length parameters are chosen as geometric progression [44].

It has been shown that this model reproduces well the basic properties of ^{6}He [20]. However, as is well known as the underbinding problem, the three-body model without the three-body interaction cannot reproduce the experimental binding energy (0.975 MeV) of the ground state of ^{6}He. The theoretical result (0.784 MeV) is lower by about 200 keV as discussed in our previous analysis [20]. This underbinding has been studied as a result of a frozen ^{4}He core assumption. By taking into account the excitation or the dissociation of the ^{4}He core, this underbinding problem in ^{6}He is believed to be solved [45,46].

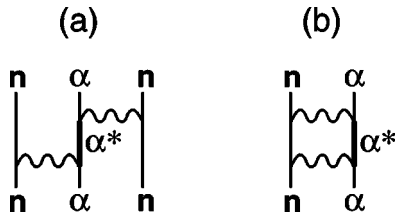

FIG. 1. (a) Diagram of the three-body interaction between ^{4}He-n-n. (b) Diagram of the two-body interaction between ^{4}He-n.

In the present study, as mentioned above, in order to overcome the underbinding problem, we introduce the three-body interaction assuming a single Gaussian function to fit the experimental binding energy and the rms radius of the ^{6}He ground state

$$V^3_{\alpha nn} = V_3 e^{-\nu(\mathbf{r}_1^2+\mathbf{r}_2^2)}, \quad V_3 = -0.218 \ \text{MeV},$$
$$\nu = (0.1/b_c)^2 \ \text{fm}^{-2}. \tag{4}$$

In the study of breakup reactions, it is very important to reproduce the threshold energies of three-body and two-body channels. We consider that this three-body interaction effectively represents a renormalization of the internal degree of freedom in the ^{4}He core, and the coupling of two valence neutrons with excited states of the ^{4}He core is included virtually through this interaction as shown in Fig. 1(a). The component of excited or diffused ^{4}He configurations is considered to be very small, and then we treat this effect as an effective three-body interaction eliminating the excited ^{4}He channel. The effect on the ^{4}He-n interaction shown in Fig. 1(b) is already taken into account in the effective ^{4}He-n potential fitted to the observed ^{4}He-n scattering data.

The three-body eigenstates are obtained by solving the eigenvalue problem of the complex-scaled Hamiltonian. We use 30 Gaussian basis functions for one radial component in order to stabilize the calculations for the position of resonances, distributions of continuum states and their transition matrix elements. The maximum range of Gaussian basis function is about 40 fm.

B. Complex scaling method and extended completeness relation

In CSM for the ^{4}He$+n+n$ model, we transform coordinate, momentum and wave function as

$$\mathbf{r}_i \rightarrow \mathbf{r}_i e^{i\theta}, \quad \mathbf{k}_\alpha \rightarrow \mathbf{k}_\alpha e^{-i\theta},$$
$$\Phi(\boldsymbol{\xi}) \rightarrow \Phi^\theta(\boldsymbol{\xi}) = e^{(3/2)i\theta\cdot f}\Phi(\boldsymbol{\xi}e^{i\theta}), \tag{5}$$

where $\mathbf{k}_\alpha$ is a momentum of continuum states measured from the threshold energy of each channel α such as ^{4}He$+n+n$ and ^{5}He$(3/2^-,1/2^-)+n$ (there is no physical threshold in the ^{4}He-2n channel). Here, f is a number of degrees of freedom of the system (for a three-body system $f=2$) and θ is a scaling angle to rotate the cuts of the Riemann sheets.

Using CSM, we obtain the energy eigenvalues of all bound and unbound states on a complex energy plane, governed by the ABC theorem [22]. In Fig. 2, we present an eigenvalue distribution for the ^{4}He$+n+n$ system schematically. When $\theta=0$ (without applying CSM), unbound (scattering) states are obtained on a real energy axis (gray straight line) corresponding to the cut of the Riemann sheet.

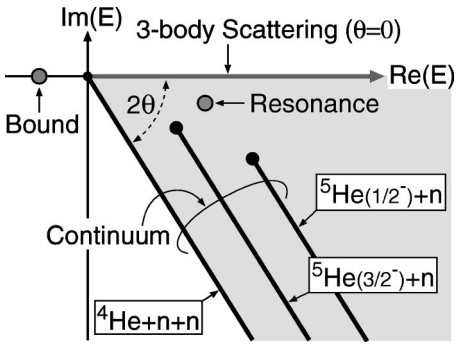

FIG. 2. Schematic distribution of energy eigenvalues of the ^{4}He$+n+n$ system with CSM where the origin of energy is chosen as the three-body threshold.

For a finite value of θ, the Riemann cuts are rotated down by 2θ and continuum states are obtained on these cuts. In the following discussions, we call these rotated continuum states simply as the continuum ones. When we take a large θ, we obtain the three-body unbound states decomposed into three categories of discrete three-body resonances, two-body continuum states of ^{5}He$(3/2^-,\ 1/2^-)+n$, and three-body continuum states of ^{4}He$+n+n$. The two-body continuum states of ^{5}He$+n$ are expressed by the two straight lines whose origins are resonance positions of ^{5}He$(3/2^-,1/2^-)$.

Using the decomposed resonances, two-body continuum, and three-body continuum states in the ^{4}He$+n+n$ system, we introduce the extended three-body completeness relation (ECR) of the complex-scaled Hamiltonian $H(\theta)$ as a natural extension of ECR in the two-body case [34–36,47–49];

$$\mathbf{1} = \sum_\nu \int |\Phi^\theta_\nu\rangle\langle\tilde{\Phi}^\theta_\nu|$$
$$= \{\text{three-body bound state of } ^6\text{He}\}$$
$$+ \{\text{three-body resonance of } ^6\text{He}\}$$
$$+ \{\text{two-body continuum states of } ^5\text{He}+n\}$$
$$+ \{\text{three-body continuum states of } ^4\text{He}+n+n\}, \tag{6}$$

where $\{\tilde{\Phi}^\theta, \Phi^\theta\}$ are complex-scaled wave functions and form a set of biorthogonal bases. As the definition of the biorthogonal bases is written in our previous papers [34,35], we only briefly explain it here. When the wave number of Φ_ν is k_ν for discrete bound and resonance states, that of $\tilde{\Phi}_\nu$ is defined as $\tilde{k}_\nu = -k^*_\nu$ that leads to the relation; $\tilde{\Phi}_\nu = (\Phi_\nu)^*$ [36]. This relation is used in the so-called c product [50] of bra and ket states in CSM. For continuum states, since we employ a discretized representation, the same rule of the biorthogonal relation of resonances is adopted.

In Eq. (6), the contours of integral for two- and three-body continuum states are taken over complex energies displayed in Fig. 2. In the ^{4}He$+n+n$ model, since n-n does not have any bound states either physical resonances, continuum states of the ^{4}He-2n channel are included in the three-body continuum component of ^{4}He$+n+n$.

C. Decomposition of the strength function

Before explanation of the strength function, we first discuss Green's function $\mathcal{G}(E,\boldsymbol{\xi},\boldsymbol{\xi}')$ in CSM, which is useful to evaluate each final state contribution in breakup reactions. Here, we define the complex-scaled Green's function $\mathcal{G}^\theta(E,\boldsymbol{\xi},\boldsymbol{\xi}')$ as follows:

$$\mathcal{G}(E,\boldsymbol{\xi},\boldsymbol{\xi}') \to \mathcal{G}^\theta(E,\boldsymbol{\xi},\boldsymbol{\xi}') = \left\langle \boldsymbol{\xi} \left| \frac{\mathbf{1}}{E-H(\theta)} \right| \boldsymbol{\xi}' \right\rangle, \tag{7}$$

$$= \sum_\nu \int \frac{\Phi^\theta_\nu(\boldsymbol{\xi})[\tilde{\Phi}^*_\nu(\boldsymbol{\xi})]^\theta}{E-E^\theta_\nu}$$

$$= \sum_\nu \int \mathcal{G}^\theta_\nu(E,\boldsymbol{\xi},\boldsymbol{\xi}'). \tag{8}$$

In derivation from Eq. (7) to Eq. (8), we insert ECR of Eq. (6). Summation and integration over ν are performed for a finite number of resonances, two-body continuum states of ^{5}He$(3/2^-,\ 1/2^-)+n$, and three-body continuum states of ^{4}He$+n+n$. There is no bound state except for the 0^+ ground state. In this expression of Green's function, E^θ_ν is the energy associated to the wave function $\Phi^\theta_\nu(\boldsymbol{\xi})$. It should be noticed that the θ dependence of E^θ_ν appears in the continuum spectra, not in discrete bound states and resonances. In addition to the initial state, all kinds of final states of the ^{4}He$+n+n$ system are obtained by solving the eigenvalue problem with a common value of θ.

The transition strength function for the operator $\hat{O}_\lambda$ with rank λ is defined in usual cases without CSM as follows:

$$\mathcal{S}_\lambda(E) = \sum_\nu \int \langle \tilde{\Phi}_i | \hat{O}^\dagger_\lambda | \Phi_\nu \rangle \langle \tilde{\Phi}_\nu | \hat{O}_\lambda | \Phi_i \rangle \delta(E-E_\nu), \tag{9}$$

$$= -\frac{1}{\pi} \mathrm{Im} \left[\int d\boldsymbol{\xi} d\boldsymbol{\xi}' \tilde{\Phi}^*_i(\boldsymbol{\xi}) \hat{O}^\dagger_\lambda \mathcal{G}(E,\boldsymbol{\xi},\boldsymbol{\xi}') \hat{O}_\lambda \Phi_i(\boldsymbol{\xi}') \right]. \tag{10}$$

We operate the complex scaling on the transition strength function of Eq. (10) and insert the complex-scaled Green's function of Eq. (8), where the physical quantity $\mathcal{S}_\lambda(E)$ itself is invariant under the complex scaling:

$$\mathcal{S}_\lambda(E) = -\frac{1}{\pi} \mathrm{Im} \left[\int d\boldsymbol{\xi} d\boldsymbol{\xi}' [\tilde{\Phi}^*_i(\boldsymbol{\xi})]^\theta (\hat{O}^\dagger_\lambda)^\theta \times \mathcal{G}^\theta(E,\boldsymbol{\xi},\boldsymbol{\xi}') \hat{O}^\theta_\lambda \Phi^\theta_i(\boldsymbol{\xi}') \right], \tag{11}$$

$$= \sum_\nu \int \mathcal{S}_{\lambda,\nu}(E). \tag{12}$$

Thus, the transition strength function is decomposed into each component $\mathcal{S}_{\lambda,\nu}(E)$ for the final state ν as

$$\mathcal{S}_{\lambda,\nu}(E) \equiv -\frac{1}{\pi} \mathrm{Im} \left[\frac{\langle \tilde{\Phi}^\theta_i | (\hat{O}^\dagger_\lambda)^\theta | \Phi^\theta_\nu \rangle \langle \tilde{\Phi}^\theta_\nu | \hat{O}^\theta_\lambda | \Phi^\theta_i \rangle}{E-E^\theta_\nu} \right]. \tag{13}$$

Due to this decomposition of unbound final states, we can unambiguously investigate which state affects the structure of the transition strength function. This is a prominent point of the present method.

Here, it should be noticed that the total transition strength $\mathcal{S}_\lambda(E)$ defined in Eq. (9) being an observable, it is positive definite for any energy and λ value. On the other hand, the partial strength $\mathcal{S}_{\lambda,\nu}(E)$ given in Eq. (13), such as a three-body resonance component, is not necessarily positive definite at all energies. This means that $\mathcal{S}_{\lambda,\nu}(E)$ can have sometimes negative values. This property of the partial strength function taking negative values are understood as follows: Since the complex-scaled Hamiltonian is non-Hermitian, and since resonances and continuum states are solved as eigenstates for complex energy eigenvalues, transition matrix elements $\langle \tilde{\Phi}^\theta_\nu | \hat{O}^\theta_\lambda | \Phi^\theta_i \rangle$ of these states are also complex numbers. The strength function for the final state ν is given by the imaginary part of the squared value of transition matrix elements, not of absolute ones for a Hermite operator $\hat{O}_\lambda$ as shown in Eq. (13). Therefore, negative values may occur in the partial transition strength function $\mathcal{S}_{\lambda,\nu}(E)$. In general, a negative distribution in $\mathcal{S}_{\lambda,\nu}(E)$ frequently appears when ν is a broad resonance that has a large resonance width and a large imaginary part of the transition matrix element. Furthermore, when negative values appear in $\mathcal{S}_{\lambda,\nu}(E)$ for continuum states, it is considered that its origin comes from resonance poles that have very large imaginary energies and are located below the continuum states (rotated Riemann cuts).

The stability of the calculation of transition matrix elements for resonances using CSM has been already checked in our previous papers [33–35]. For continuum states, we adopt the discretized representation and evaluate the transition matrix between them as for resonances. To see the reliability of discretization of continuum states, we checked the transition strength by changing parameters of the Gaussian basis functions. In those calculations, we see negligible changes in the calculated transition strength, and then we consider that the representation of continuum states in our model gives a good approximation quantitatively. This stability of the matrix elements for continuum states seems to come from the fact that we solve continuum states with a large basis set to describe their spatially extended behavior.

TABLE I. Results of the binding energy of the ground state, positions of resonances (E_r,Γ) (unit in MeV) and matter radius (unit in fm) in our model and experimental data of them [51,53–55].

	Ref. [20]	Present	Main component	Experiment
0_1^+	0.784	0.975	$(p_{3/2})^2$	0.975 [a]
2_1^+	(1.02, 0.26)	(0.81, 0.13)	$(p_{3/2})^2$	$(0.822\pm 25,\ 0.113\pm 20)$ [a]
2_2^+	(2.64, 4.75)	(2.35, 4.22)	$(p_{3/2})(p_{1/2})$	
1^+	(2.98, 6.39)	(2.67, 6.13)	$(p_{3/2})(p_{1/2})$	
0_2^+	(3.91, 9.45)	(3.69, 9.14)	$(p_{1/2})^2$	
R_m	2.50	2.46		2.48 ± 0.03 [b]
				2.33 ± 0.04 [c]
				2.50 [d]

[a]Reference [51].
[b]Reference [53].
[c]Reference [54].
[d]Reference [55].

III. RESULTS

First we compare the present spectroscopic results of ^{6}He with the previous ones [20]. In Table I, we list the binding energy of the ground state, the energies and resonance widths of the 2_1^+, and predicted resonances; (E_r,Γ), main components of each level, and matter radius of the ground state in comparison with experimental data. We can see a good agreement between our calculations and experimental data. The present calculation does not predict 1^- resonances in the low excitation energy region in agreement with the previous one [20]. This result is consistent with the experimental situation [51,52]. In our calculation, the occupation probability of $(p_{3/2})^2$ in the ground state is 90.2%, and other levels are also mainly described by p^2 configurations of two valence neutrons. This indicates that the j-j coupling scheme is well established in ^{6}He over this energy region. It is found that the three-body interaction noticeably improves the position of the 2_1^+ state. For other resonances, the energies and widths in the present calculation are lower by about few hundred keV than in the previous one [20]. The whole energy level scheme of ^{6}He is displayed in Fig. 3.

Next, we investigate the contributions in the electric multipole transition strengths not only from the three-body resonances, but also from the two-body continuum states of ^{5}He$+n$ and the three-body continuum states of ^{4}He$+n+n$. The transition strength corresponds to the reduced transition strength distribution $dB(E\lambda)/dE$ where λ is the multipolarity. We analyze which components dominate the observed behavior of the strength distribution in each multipolarity.

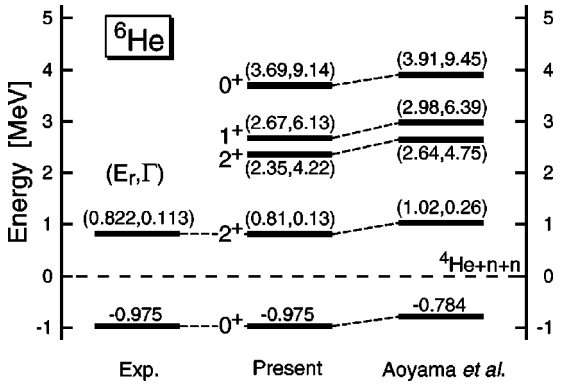

FIG. 3. Energy levels of ^{6}He. Unit of energies and resonance widths is MeV.

A. $E1$ transitions

In Fig. 4, we show the eigenvalue distribution for 1^- states. This result is obtained by diagonalization of the complex-scaled Hamiltonian of the ^{4}He$+n+n$ model with $\theta=35°$. As basis states of COSM, we used s-, p-, and d-waves between ^{4}He and each valence neutron, because it is confirmed that the effect of other higher partial waves is very small in the transition strength. From Fig. 4, we see that all eigenvalues are obtained along three lines of rotated Riemann cuts corresponding to two two-body and one three-body continuum channels. There is no 1^- resonance. Therefore, these results indicate that the 1^- unbound states above the ^{4}He$+n+n$ threshold are classified into two-body continuum states of ^{5}He$(3/2^-,1/2^-)+n$ and three-body continuum states of ^{4}He$+n+n$.

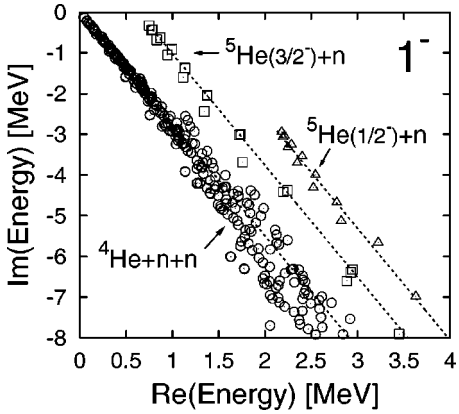

FIG. 4. Energy eigenvalues of 1^- states calculated with CSM where θ is 35°. Squares and triangles indicate the two-body continuum states of ^{5}He$(3/2^-)+n$ and ^{5}He$(1/2^-)+n$, respectively. Circles indicate the three-body continuum states of ^{4}He$+n+n$.

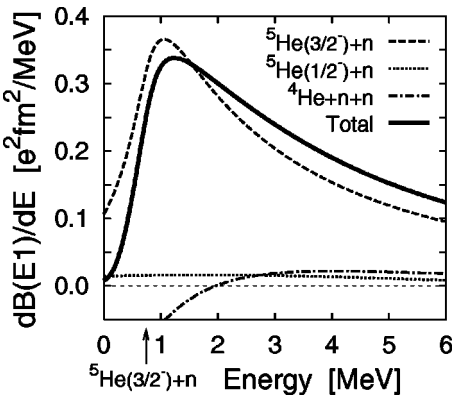

FIG. 5. $E1$ transition strength distributions where dashed, dotted, and dash-dotted lines are contributions from the two- and three-body continuum states. The thick solid line indicates the total strength distribution. The position of the arrow stands for the two-body threshold energy of the $^5\mathrm{He}(3/2^-)+n$ channel.

Using these solutions, we calculate the transition strength from the ground state to all components of 1^- states. The calculated $E1$ transition strength distribution is displayed in Fig. 5. It is found that there is a low energy enhancement in the total strength at around 1 MeV measured from the three-body threshold energy. This energy is just above the two-body threshold (0.74 MeV) of $^5\mathrm{He}(3/2^-)+n$ [20], and the $E1$ transition strength slowly decreases with the excitation energy. The most interesting result is that the dominant transition strength comes from the two-body continuum component of $^5\mathrm{He}(3/2^-)+n$ showing the low energy enhancement, and that contributions from the other components are relatively very small. This result indicates that the three-body Coulomb breakup strength of ^{6}He is dominated by the sequential breakup of a $^6\mathrm{He}\rightarrow{}^5\mathrm{He}+n\rightarrow{}^4\mathrm{He}+n+n$ process. It is consistent with the discussion of the observed invariant mass spectrum of the ^{4}He-n system [8,12,14].

Our calculated $E1$ distribution is very similar to that of Danilin *et al.* [18] where there is a low energy enhancement in the transition strength. On the other hand, the experimental data [8] do not show a sharp enhancement in the low excitation energy region. However, the error bars in the experimental data are rather large. Further experimental data are desired.

We investigate more detailed structures of the $E1$ transition strength from two points of view; configurations of the initial ground state and 1^- final ones of ^{6}He. The first point is to see the relation between the structure of the ground state and the $E1$ transition strength. Although $^5\mathrm{He}(3/2^-)$ is a resonance, the wave function of $^5\mathrm{He}(3/2^-)$ in the $^5\mathrm{He}(3/2^-)+n$ channel has a large overlap with the $^4\mathrm{He}+n_{p_{3/2}}$ configuration that is a dominant component in the ^{6}He ground state. The result of the large transition strength into the $^5\mathrm{He}(3/2^-)+n$ channel indicates that one of the neutrons of $(p_{3/2})^2$ in the ^{6}He ground state is excited to a continuum state of s- or d-wave orbit by the $E1$ external field. Furthermore, we can see that the three-body continuum states of $^4\mathrm{He}+n+n$ do not contribute strongly. This result indicates that two $p_{3/2}$-orbital neutrons in the ^{6}He ground state are hardly excited simultaneously in the breakup reaction. Another two-body continuum component of $^5\mathrm{He}(1/2^-)+n$ hardly contributes to the strength because the probability of $(p_{1/2})^2$ is very small in the ground state, nearly a few percent. Furthermore, a large resonance width (5.84 MeV) of $^5\mathrm{He}(1/2^-)$ also reduces and broadens the strength, and then we cannot see a distinguishable structure of the two-body component of $^5\mathrm{He}(1/2^-)+n$ in the $E1$ transition strength.

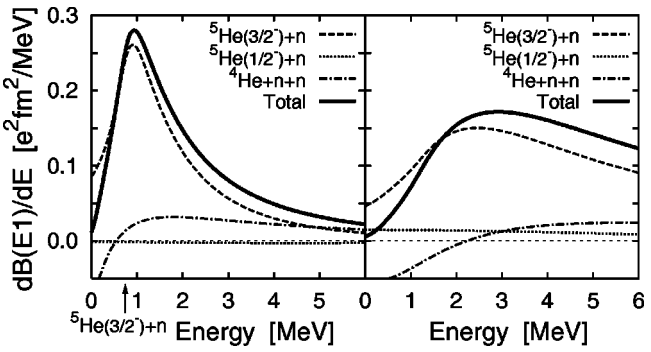

FIG. 6. $E1$ transition strength distributions with limited 1^- configurations. The left panel shows $(^4\mathrm{He}+n_p)+n_s$ configurations where subscript means the orbital angular momentum of each valence neutron. The right panel shows $(^4\mathrm{He}+n_p)+n_d$ configurations.

The second point is to see what kinds of final-state configurations give large contributions to the strength function. For this purpose, we calculate the transition components of dominant 1^- final-state configurations such as $(p_{3/2},s_{1/2})$, $(p_{3/2},d_{3/2,5/2})$, $(p_{1/2},s_{1/2})$, or $(p_{1/2},d_{3/2,5/2})$ of two valence neutrons. When one of the valence neutrons is the p-orbital resonance, the final-state configurations are expressed as $^5\mathrm{He}(3/2^-,1/2^-)+n_{sd}$ where the subscript means the orbital angular momentum of the last neutron, because the $p_{3/2,1/2}$-orbital neutron around the ^{4}He core already forms the resonance of $^5\mathrm{He}(3/2^-,1/2^-)$. The results are shown in Fig. 6. From these results, it is found that the $^5\mathrm{He}(3/2^-)+n_s$ component gives the main contribution and makes a large enhancement at low energies in the total strength. The $^5\mathrm{He}(3/2^-)+n_d$ component also gives a large contribution and produces a broad peak around 2–3 MeV in the total strength.

As was shown above, the transition strengths are very weak for three-body continuum states of $^4\mathrm{He}+n_p+n_{sd}$, but strong for two-body continuum states of $^5\mathrm{He}(3/2^-)+n_{sd}$. Here we show that the two-body continuum states of $^5\mathrm{He}(3/2^-)+n$ are approximately described by plane waves. For the 1^- final states, we assume a free motion between the resonant $^5\mathrm{He}(3/2^-)$ nucleus and the residual neutron with the relative s- and d-angular momenta, and calculate the $E1$ transition strength from the ground state of ^{6}He to these configurations. The obtained strength distributions are shown in Fig. 7, and are very similar to the results shown in Fig. 6. Thus, the low energy enhancement is interpreted as a threshold effect of the two-body continuum in the $^5\mathrm{He}(3/2^-)+(s\text{-orbital neutron})$ channel. The similar plane-wave description of the strength distribution is seen in the breakup reaction of the one-neutron halo nucleus ^{11}Be [6]. This low-

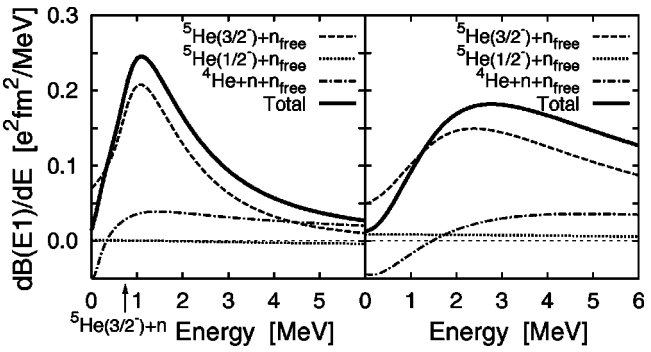

FIG. 7. $E1$ transition strength distributions with limited 1^- configurations. Any interactions for s- and d-orbital valence neutrons are cut off. The left panel is $(^4\mathrm{He}+n_p)+n_{s,\mathrm{free}}$ configurations, and the right panel is $(^4\mathrm{He}+n_p)+n_{d,\mathrm{free}}$ configurations.

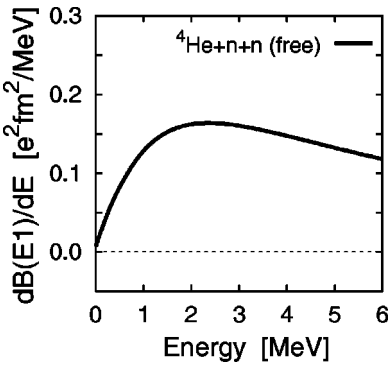

FIG. 8. $E1$ transition strength distributions without any final state interactions between clusters.

momentum peak of ^{11}Be is explained as a result of the one-neutron halo structure of the ground state. However, in the present case, since the ground state of ^{6}He has a two-neutron halo structure, the reaction process is different from that of ^{11}Be. We have the following interpretation on the $E1$ breakup process of ^{6}He: The ^{6}He nucleus is broken up to $^4\mathrm{He}+n+n$, where three particles are not free but have an interaction between ^{4}He and one neutron. Furthermore, in final 1^- states, the interacting ^{4}He and one neutron form the resonance of $^5\mathrm{He}(3/2^-)$, but the residual neutron has no interaction with the resonant ^{5}He system. The low angular momentum s- and d-components dominate and their summation almost reproduces the total transition strength of the $^5\mathrm{He}(3/2^-)+n$ breakup.

It is noticed in Figs. 5–7 that transition strength amplitudes remain even below the two-body threshold energy (0.74 MeV) in the two-body continuum component of $^5\mathrm{He}(3/2^-)+n$. This result is explained by the fact that the wave function of the $^5\mathrm{He}(3/2^-)$ resonance in the $^5\mathrm{He}(3/2^-)+n$ channel, has a spread over the energy range beyond the threshold energy due to the resonance width. Furthermore, it is found that the three-body continuum strength presents negative values in the energy region lower than 2 MeV. This result does not contradict the observation because the observed strength (the total strength) keeps positive value, as was explained in Sec. II C. The dynamical origin of negative values in the three-body continuum strength is considered to come from the existence of some broad resonance poles hidden below the three-body continuum states. The same situation appears in $E2$ transitions as shown in the next subsection.

If there are no two-body or three-body resonances with no final state interaction, the three-body continuum strength shows a positive distribution as shown in Fig. 8. The $E1$ transition strength of Fig. 8 is calculated for the three-body plane wave functions as the final states under the assumption of no interactions between all clusters. As mentioned above, this strength distribution does not include any resonance contribution that arises from the interactions between clusters. Similar calculation was also shown for ^{11}Li by Pushkin *et al.* [56]. In the calculated distribution, we see a broad enhancement with a bump at around 2 MeV. This enhancement is interpreted as a result of the halo structure of the ^{6}He ground state. If the interactions between clusters are very weak and the three-body plane wave approximation is acceptable, the $E1$ transition strength distribution may be described by the result of Fig. 8. However, as was shown above, the interaction between clusters, especially the final state interaction between ^{4}He-n, plays an important role in the 1^- final states. It is shown that the final state interaction between ^{4}He and n not only changes the shape of the strength distribution, but also increases the strength of the distribution.

B. $E2$ transitions

$E2$ transitions are also important in the low energy strength of the Coulomb breakup reaction. Its strength is expected to show a behavior very different from $E1$ transitions because there are $2^+_{1,2}$ resonances of the $^4\mathrm{He}+n+n$ system in the low excitation energy region as shown in Table I. In Fig. 9, we show the obtained $2^+_{1,2}$ resonances and continuum solutions that are decomposed into two- and three-body continuum states. Although we saw that the $E1$ transition strength distribution does not have any resonant structure, it is very interesting to see the resonant contribution in the $E2$ transition strength.

Before discussing the results of the $E2$ transition strength distribution into three-body unbound states, we show the

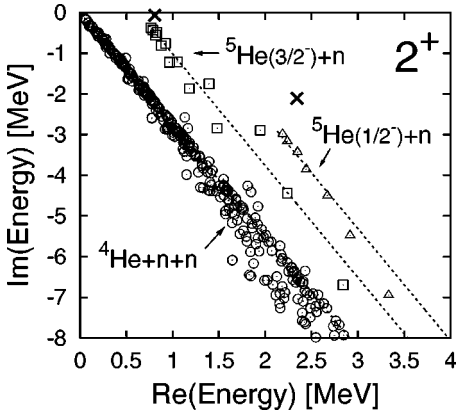

FIG. 9. Energy eigenvalues of 2^+ states calculated with CSM where two crosses are $2^+_{1,2}$ resonances and other marks indicate the same meanings as those in Fig. 4.

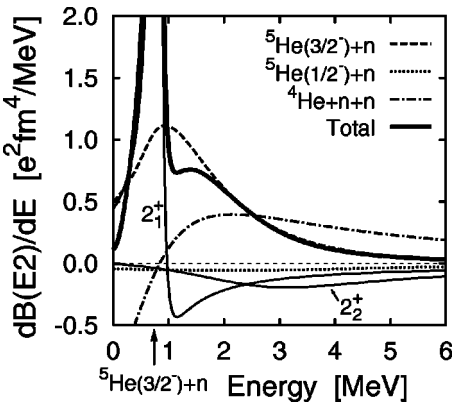

FIG. 10. $E2$ transition strength distributions where two thin solid lines are the contributions from $2^+_{1,2}$ resonances and dashed, dotted, and dash-dotted lines are those from the two- and three-body continuum states. Thick solid line indicates the total strength distribution.

transition matrix elements between the initial ground state and $2^+_{1,2}$ resonances, whose squared values [transition strengths $B(E2)$] are $2.78+i0.43$ for 2^+_1 and $-1.5+i0.9$ for 2^+_2, respectively (units in $e^2\,\mathrm{fm}^4$). Transition strengths are obtained as complex numbers, as well as the eigenvalue of energies. It is found that the absolute values of the transition strengths of 2^+_1 and 2^+_2 resonances are of the same order because the configurations of $2^+_{1,2}$ are dominantly described by the common p orbitals. One must be careful to compare the calculated complex values with observations [57], because what we observe is for scattering states, not for pure resonances of complex energies. However, for the 2^+_1 resonance, the large real part of the transition strength in comparison with the imaginary one seems to correspond to the experimental value $3.2\pm0.6\,e^2\,\mathrm{fm}^4$ reported by Aumann *et al.* [8]. When the resonance pole is very close to the real energy axis, its matrix elements show large real parts that may correspond well with observables. On the other hand, the 2^+_2 resonance has a large resonance width (4.22 MeV) and a large imaginary part of the transition strength. Then, it may be difficult to correspond directly its transition strength with the observable.

The obtained $E2$ transition strength distribution including resonance and continuum states is displayed in Fig. 10. There are five kinds of components: transitions to $2^+_{1,2}$ resonances, two-body continuum states of $^5\mathrm{He}(3/2^-,1/2^-)+n$, and three-body continuum ones of $^4\mathrm{He}+n+n$. From Fig. 10, we can see that the 2^+_1 resonance gives the main contribution showing a sharp peak around the resonance energy (0.81 MeV) due to the small resonance width. On the other hand, the contribution from the 2^+_2 resonance is very small due to the large width in comparison with the 2^+_1 resonance, in spite of the same order of the transition matrix elements. The components associated to two-, or three-body continua are smaller than those of 2^+_1. However, in the continuum transitions, the two-body continuum component of $^5\mathrm{He}(3/2^-)+n$ shows a peak at around 1 MeV, just above the two-body threshold energy of this channel. This component mainly contributes to make a shoulder in the total strength at around 1.5 MeV measured from the $^4\mathrm{He}+n+n$ threshold energy. The reason why the two-body component of $^5\mathrm{He}(3/2^-)+n$ makes a peak at around 1 MeV is as follows: This two-body component consists of $^5\mathrm{He}(3/2^-)+(p$-orbital continuum neutron) channels dominantly due to orthogonality to the 2^+_1 and 2^+_2 resonances. Furthermore, we can confirm that this p-orbital continuum neutron has a similar structure to the p-orbital plane wave, and a peak at around 1 MeV is interpreted as a two-body threshold effect as in the case of the $E1$ transition.

The effect of another two-body continuum component of $^5\mathrm{He}(1/2^-)+n$ is very small as well as the case of the $E1$ transition. It is found that the three-body continuum component of $^4\mathrm{He}+n+n$ relatively gives a larger contribution than the case of $E1$ transition. This three-body component also contributes to make a shoulder at around 1.5 MeV in the total transition strength. A similar structure was obtained by Danilin *et al.* [18], though their shoulder structure is more isolated and has a larger strength. This difference of the shoulder behavior from our result may come from the rather small resonance width of the 2^+_2 resonance in comparison with our result.

In the present calculation, it is found that the $E2$ transition strength distribution shows a distinguishable resonance behavior of the 2^+_1 state, but not of the 2^+_2 state directly. It may be hard to observe experimentally the existence of the 2^+_2 state by using Coulomb breakup reactions. On the other hand, the continuum strengths consisting of $^5\mathrm{He}(3/2^-)+n$ and $^4\mathrm{He}+n+n$ channels make a shoulderlike structure. Through an observation of this structure, the continuum effect is expected to be confirmed in the $E2$ transition strength in addition to that of resonances.

C. Cross section

We calculate the Coulomb dissociation cross section by using $E1$ and $E2$ transition strengths obtained in the former subsections. The cross section is expressed by multiplying the reduced transition probability $dB(E\lambda,E)/dE$ and the virtual photon number $N_{E\lambda}(E)$ from the equivalent photon method [58,59]. In Fig. 11, we show the calculated cross section in comparison with the experimental one, where target is Pb and the incident energy of ^{6}He projectile is 240 MeV/nucleon. In this calculation the minimum value of the impact parameter is taken as 12 fm. We also calculate the convoluted cross section in addition to the original one. The parameter set for the convolution with respect to the energy resolution and detector response is the same as used in Ref. [8].

The whole shape of our cross section is very similar to the experimental data except for the too large peak at around 1 MeV that is mainly coming from the $E1$ component. It is found that the $E2$ component is quite small and that its structure cannot be seen in the total cross section even if there is a 2^+_1 resonance. Of course our result does not include the nuclear interaction at this stage, however, our analysis shows that the contribution from the $E1$ transition strength dominantly determines the shape of the dissociation cross section

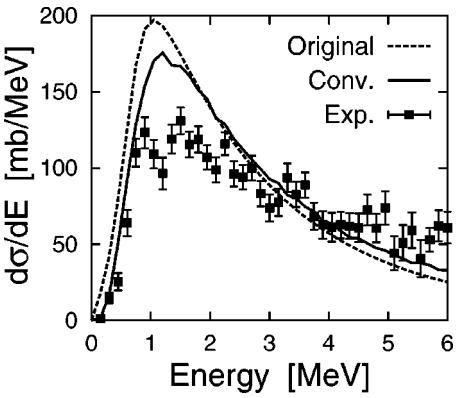

FIG. 11. Coulomb dissociation cross sections of ^{6}He into the $^4\mathrm{He}+n+n$ system with and without the convolution. Experimental data are taken from Ref. [8].

in the low excitation energy region, though there is no 1^- resonance.

IV. SUMMARY

We analyzed the structure of three-body unbound states in the two-neutron halo nucleus ^{6}He, by focusing on the transition strength of the Coulomb breakup reaction. In addition to the halo structure in the ground state, the understanding of three-body unbound $^4\mathrm{He}+n+n$ states is important to clarify the excitation mechanism of ^{6}He concerning breakup reactions.

In the study of the transition strength of three-body breakup reactions, it is necessary to determine the associated resonances and continuum states simultaneously, and to examine the role of each state. In order to describe the three-body unbound states of ^{6}He with the $^4\mathrm{He}+n+n$ model, we employed the complex scaling method (CSM). It has been shown that CSM is useful to solve resonances and continuum states in a unified framework. We also used the complex-scaled Green's function [Eq. (8)], where we applied the extended completeness relation (ECR) to decompose the transition strengths into every components of the unbound states. It was verified that CSM works successfully to evaluate the transition strengths of the three-body system beyond the two-body case.

In this paper, through the decomposition of the transition strength into three-body resonances, and two- and three-body continuum components, we carefully investigated the detailed structures in the characteristic distribution of the transition strength of ^{6}He. It was found that for the $E1$ transition strength, the sequential breakup process through the $^5\mathrm{He}(3/2^-)+n$ channel is mostly favored rather than other processes, and makes a low energy enhancement due to the two-body threshold effect. For the $E2$ transition strength, in addition to the contributions of the $2^+_{1,2}$ resonances, those from the continuum states were calculated separately. We found two kinds of structures (peak and shoulder) in the calculated strength; one comes from the contribution from 2^+_1 resonance, and another from the two- and the three-body continuum components. In the Coulomb dissociation cross section consisting of $E1$ and $E2$ dominantly, it is not possible to see the detailed structures of the $E2$ transition because of much larger $E1$ transition.

Based on the present successful results, we are going to extend this method to the analysis of an influence from the nuclear interaction in the breakup reaction of ^{6}He. It is also interesting to apply the present approach to other types of reactions such as charge exchange with ^{6}Li, proton scattering and so on. In these reactions, we may see the different contributions of resonance and continuum states of ^{6}He from the case of the Coulomb excitation. The knowledge obtained from these reactions is important in manifesting the varieties of the structure of the unbound states of ^{6}He. We also have a plan to study the breakup reactions of other unstable nuclei such as ^{11}Li. Since the ^{11}Li nucleus is suggested to have a large mixture of s waves in the ground state [60,61], unlike the case of ^{6}He, it is very interesting to investigate the possibility of a soft-dipole resonance.

ACKNOWLEDGMENTS

The authors would like to acknowledge valuable discussions with Professor A. Ohnishi. The authors also would like to thank the members of the nuclear theory group in Hokkaido University for their kind interest and discussions. The authors thank Professor T. Aumann for giving us the experimental data of the cross section and the code to derive the convoluted one. Computational calculations of this work were supported by Hokkaido University Computing Center, Division of Physics of Hokkaido University and Research Center for Nuclear Physics (RCNP) of Osaka University. This work was supported by the Grant-in-Aid for Scientific Research (Grant No. 12640246) of the Ministry Education, Science and Culture, Japan.

[1] I. Tanihata, H. Hamagaki, O. Hashimoto, Y. Shida, N. Yoshikawa, K. Sugimoto, O. Yamakawa, T. Kobayashi, and N. Takahashi, Phys. Rev. Lett. **55**, 2676 (1985).
[2] I. Tanihata, Nucl. Phys. **A488**, 113c (1988).
[3] I. Tanihata, J. Phys. G **22**, 157 (1996).
[4] P. G. Hansen and B. Jonson, Europhys. Lett. **4**, 409 (1987).
[5] K. Ikeda, Nucl. Phys. **A538**, 355c (1992).
[6] T. Nakamura *et al.*, Phys. Lett. B **331**, 296 (1994).
[7] T. Nakamura *et al.*, Phys. Rev. Lett. **83**, 1112 (1999).
[8] T. Aumann *et al.*, Phys. Rev. C **59**, 1252 (1999).
[9] K. Ieki *et al.*, Phys. Rev. Lett. **70**, 730 (1993); D. Sackett *et al.*, Phys. Rev. C **48**, 118 (1993).
[10] S. Shimoura, T. Nakamura, M. Ishihara, N. Inabe, T. Kobayashi, T. Kubo, R. H. Siemssen, I. Tanihata, and Y. Watanabe, Phys. Lett. B **348**, 29 (1995).
[11] M. Zinser *et al.*, Nucl. Phys. **A619**, 151 (1997).
[12] T. Kobayashi, Riken preprint RIKEN-AF-NP-158, 1993 (unpublished).

[13] L. V. Chulkov *et al.*, Phys. Rev. Lett. **79**, 201 (1997).
[14] D. Aleksandrov *et al.*, Nucl. Phys. **A633**, 234 (1998).
[15] F. M. Nunes, I. J. Thompson, and R. C. Johnson, Nucl. Phys. **A596**, 171 (1996).
[16] P. Descouvemont, Nucl. Phys. **A615**, 261 (1997).
[17] M. V. Zhukov, B. V. Danilin, D. V. Fedorov, J. M. Bang, I. J. Thompson, and J. S. Vaagen, Phys. Rep. **231**, 151 (1993).
[18] B. V. Danilin, I. J. Thompson, J. S. Vaagen, and M. V. Zhukov, Nucl. Phys. **A632**, 383 (1998).
[19] A. Cobis, D. V. Fedorov, and A. S. Jensen, Phys. Rev. Lett. **79**, 2411 (1997); Phys. Rev. C **58**, 1403 (1998).
[20] S. Aoyama, S. Mukai, K. Katō, and K. Ikeda, Prog. Theor. Phys. **93**, 99 (1995); **94**, 343 (1995).
[21] S. Aoyama, K. Katō, and K. Ikeda, Phys. Rev. C **55**, 2379 (1997).
[22] J. Aguilar and J. M. Combes, Commun. Math. Phys. **22**, 269 (1971); E. Balslev and J. M. Combes, *ibid.* **22**, 280 (1971).
[23] A. T. Kruppa, R. G. Lovas, and B. Gyarmati, Phys. Rev. C **37**, 383 (1988).
[24] A. T. Kruppa and K. Katō, Prog. Theor. Phys. **84**, 1145 (1990).
[25] K. Katō and K. Ikeda, Prog. Theor. Phys. **89**, 623 (1993).
[26] M. Teshigawara, K. Katō, and G. F. Filippov, Prog. Theor. Phys. **92**, 79 (1994).
[27] A. Csótó, Phys. Rev. C **49**, 2244 (1994).
[28] A. Csótó, Phys. Rev. C **49**, 3035 (1994).
[29] S. Aoyama, K. Katō, and K. Ikeda, Phys. Lett. B **414**, 13 (1997).
[30] S. Aoyama, N. Itagaki, K. Katō, and K. Ikeda, Phys. Rev. C **57**, 975 (1998).
[31] S. Aoyama, K. Katō, and K. Ikeda, Prog. Theor. Phys. **99**, 623 (1998).
[32] K. Katō, T. Yamada, and K. Ikeda, Prog. Theor. Phys. **101**, 119 (1999).
[33] M. Homma, T. Myo, and K. Katō, Prog. Theor. Phys. **97**, 561 (1997).
[34] T. Myo and K. Katō, Prog. Theor. Phys. **98**, 1275 (1997).
[35] T. Myo, A. Ohnishi, and K. Katō, Prog. Theor. Phys. **99**, 801 (1998).
[36] T. Berggren, Nucl. Phys. **A109**, 265 (1968).
[37] H. Kanada, T. Kaneko, S. Nagata, and M. Nomoto, Prog. Theor. Phys. **61**, 1327 (1979).
[38] Y. C. Tang, M. LeMere, and D. R. Thompson, Phys. Rep. **47**, 167 (1978).
[39] V. I. Kukulin, V. M. Krasnopol'sky, V. T. Voronchev, and P. B. Sazonov, Nucl. Phys. **A453**, 365 (1986).
[40] Y. Tosaka, Y. Suzuki, and K. Ikeda, Prog. Theor. Phys. **83**, 1140 (1990).
[41] S. Mukai, S. Aoyama, K. Katō, and K. Ikeda, Prog. Theor. Phys. **99**, 381 (1998).
[42] Y. Suzuki and K. Ikeda, Phys. Rev. C **38**, 410 (1988).
[43] Y. Suzuki and Wang Jing Ju, Phys. Rev. C **41**, 736 (1990).
[44] M. Kamimura, Phys. Rev. A **38**, 621 (1988); H. Kameyama and M. Kamimura, and Y. Fukushima, Phys. Rev. C **40**, 974 (1989).
[45] A. Csótó, Phys. Rev. C **48**, 165 (1993).
[46] K. Arai, Y. Suzuki, and R. G. Lovas, Phys. Rev. C **59**, 1432 (1999).
[47] T. Berggren and P. Lind, Phys. Rev. C **47**, 768 (1992).
[48] T. Vertse, P. Curutchet, and R. J. Liotta, Phys. Rev. C **42**, 2605 (1990).
[49] T. Vertse, R. J. Liotta, and E. Maglione, Nucl. Phys. **A584**, 13 (1994).
[50] N. Moiseyev, P. R. Certain, and F. Weinhold, Mol. Phys. **36**, 1613 (1978).
[51] F. Ajzenberg-selove, Nucl. Phys. **A506**, 1 (1989).
[52] J. Jänecke *et al.*, Phys. Rev. C **54**, 1070 (1996).
[53] I. Tanihata, T. Kobayashi, O. Yamakawa, S. Shimoura, K. Ekuni, K. Sugimoto, N. Takahashi, T. Shimoda, and H. Sato, Phys. Lett. B **206**, 592 (1988).
[54] I. Tanihata, D. Hirata, T. Kobayashi, S. Shimoura, K. Sugimoto, and H. Toki, Phys. Lett. B **289**, 261 (1992).
[55] J. S. Al-Khalili and J. A. Tostevin, Phys. Rev. C **57**, 1846 (1997).
[56] A. Pushkin, B. Jonson, and M. V. Zhukov, J. Phys. G **22**, L95 (1996).
[57] T. Berggren, Phys. Lett. **33B**, 547 (1970); Phys. Lett. B **373**, 1 (1996).
[58] B. Hoffmann and G. Baur, Phys. Rev. C **30**, 247 (1984).
[59] C. A. Bertulani and G. Baur, Phys. Rep. **163**, 299 (1988).
[60] F. C. Barker and G. T. Hickey, J. Phys. G **3**, L23 (1977).
[61] I. J. Thompson and M. V. Zhukov, Phys. Rev. C **49**, 1904 (1994).